Coordinated regulation of sulfur and phospholipid metabolism reflects the importance of methylation in the growth of yeast

Mark J. Hickman[a,*], Allegra A. Petti[a,*], Olivia Ho-Shing[a], Sanford J. Silverman[a], R. Scott McIsaac[a], Traci A. Lee[b], and David Botstein[a]

[a]Lewis-Sigler Institute for Integrative Genomics and Department of Molecular Biology, Princeton University, Princeton, NJ 08544; [b]Biological Sciences, University of Wisconsin–Parkside, Kenosha, WI 53141

ABSTRACT **A yeast strain lacking Met4p, the primary transcriptional regulator of the sulfur assimilation pathway, cannot synthesize methionine. This apparently simple auxotroph did not grow well in rich media containing excess methionine, forming small colonies on yeast extract/peptone/dextrose plates. Faster-growing large colonies were abundant when overnight cultures were plated, suggesting that spontaneous suppressors of the growth defect arise with high frequency. To identify the suppressor mutations, we used genome-wide single-nucleotide polymorphism and standard genetic analyses. The most common suppressors were loss-of-function mutations in *OPI1*, encoding a transcriptional repressor of phospholipid metabolism. Using a new system that allows rapid and specific degradation of Met4p, we could study the dynamic expression of all genes following loss of Met4p. Experiments using this system with and without Opi1p showed that Met4 activates and Opi1p represses genes that maintain levels of *S*-adenosylmethionine (SAM), the substrate for most methyltransferase reactions. Cells lacking Met4p grow normally when either SAM is added to the media or one of the SAM synthetase genes is overexpressed. SAM is used as a methyl donor in three Opi1p-regulated reactions to create the abundant membrane phospholipid, phosphatidylcholine. Our results show that rapidly growing cells require significant methylation, likely for the biosynthesis of phospholipids.**

Monitoring Editor
Charles Boone
University of Toronto

Received: May 31, 2011
Revised: Aug 11, 2011
Accepted: Aug 31, 2011

INTRODUCTION

In the yeast *Saccharomyces cerevisiae*, the reactions and enzyme-encoding genes of several metabolic pathways, like the sulfur and phospholipid pathways studied here, have been identified and partially characterized. Studies of synthetic interactions between genes have sought to identify higher-order, indirect interactions between biological pathways (Tong *et al.*, 2001). Data from these studies have enabled the creation of quantitative models that integrate yeast metabolism and transcriptional regulation (Herrgard *et al.*, 2006). However, our understanding of the yeast cell is still incomplete, as exemplified by the fact that no existing model is able to perfectly predict the in vivo response of a cell to external stimuli or genetic perturbations (Zomorrodi and Maranas, 2010). One possible reason for this failure is that many genes have multiple cellular roles and participate in indirect or condition-specific genetic interactions that are difficult to identify and understand mechanistically. Likewise, many metabolites participate in multiple reactions, leading to complex connections between metabolic pathways.

One example is the sulfur assimilation pathway, which is a critical and ancient pathway present in all microbes and eukaryotes. This pathway incorporates extracellular sulfate into several key sulfur-containing compounds, including methionine, cysteine, homocysteine, and *S*-adenosylmethionine (SAM). The activity of this pathway has widespread influence on other cellular pathways, largely because SAM is required for most methyl transfer reactions (Thomas and Surdin-Kerjan, 1997). Accordingly, the biosynthetic genes of the sulfur assimilation pathway are controlled by a complex regulatory system that maintains the sulfur-containing compounds at

This article was published online ahead of print in MBoC in Press (http://www.molbiolcell.org/cgi/doi/10.1091/mbc.E11-05-0467) on September 7, 2011.

*These authors contributed equally to this work.

Address correspondence to: Mark J. Hickman (hickmanm@tcnj.edu), Allegra A. Petti (apetti@princeton.edu), David Botstein (botstein@genomics.princeton.edu).

Abbreviations used: PC, phosphatidylcholine; SAM, *S*-adenosylmethionine; SNP, single-nucleotide polymorphism.

appropriate levels (Lee *et al.*, 2010). At the center of this regulatory system is the transcriptional activator Met4p, which is recruited to specific promoters by the site-specific DNA-binding cofactors Met31, Met32, and Cbf1 (Thomas and Surdin-Kerjan, 1997; Lee *et al.*, 2010).

Transcriptional regulation occurs primarily at the level of Met4p activity, which is negatively regulated by SAM (Thomas *et al.*, 1988; Kuras and Thomas, 1995), creating a negative feedback loop that decreases sulfur assimilation when its products are sufficiently abundant. When SAM is abundant, Met4p is ubiquitinated, which, depending on other conditions, either leads to Met4p degradation by the proteasome or a change in Met4p activity (Kaiser *et al.*, 2000; Rouillon *et al.*, 2000; Kuras *et al.*, 2002; Flick *et al.*, 2004; Chandrasekaran *et al.*, 2006). Besides controlling methionine metabolism, Met4p, when artificially overexpressed, causes a G_1-S arrest, suggesting that Met4p mediates a cell cycle checkpoint ensuring that cells contain sufficient levels of metabolites before embarking toward cell division (Patton *et al.*, 2000).

In this study, we found that the sulfur assimilation pathway genetically interacts with another metabolic pathway, the phospholipid biosynthesis pathway. Phospholipids, such as phosphatidylcholine (PC), make up a large fraction of membrane bilayers. The enzymatic genes of this pathway are repressed by Opi1p, a protein that directly senses the levels of phosphatidic acid (PA), a precursor of phospholipid biosynthesis. When the levels of PA are low because PA has been consumed by phospholipid biosynthesis, Opi1p represses transcription by inhibiting, through an unknown mechanism, the DNA-binding transcriptional activators Ino2p and Ino4p (White *et al.*, 1991; Santiago and Mamoun, 2003; Loewen *et al.*, 2004; Jesch *et al.*, 2005). Of interest, there is a metabolic connection between sulfur assimilation and phospholipid biosynthesis; PC is biosynthesized de novo from another phospholipid, phosphatidylethanolamine, in three steps that require SAM, formed by the sulfur assimilation pathway (Chin and Bloch, 1988).

Deleting *MET4* results in methionine auxotrophy (Masselot and De Robichon-Szulmajster, 1975) because Met4p is required for the expression of many of the biosynthetic *MET* genes (Lee *et al.*, 2010). Although there is no doubt that Met4p is required for methionine biosynthesis, there is conflicting evidence (described in Table 1) about whether Met4p is required for growth in the presence of exogenous methionine. Here we found that a *met4*Δ strain does indeed have a severe growth defect, suggesting that Met4p has a function in addition to regulating *MET* genes. Furthermore, we found that suppressors of the growth defect of a *met4*Δ strain arise very frequently. To understand how *met4*Δ growth is impaired, we used genome-wide tiling arrays, sequencing, and standard genetic analysis to characterize the suppressor mutations. We found that the suppression was most often caused by loss-of-function mutations in *OPI1*. Expression microarray studies using a Met4p-degradation system showed that Met4p activates genes involved in producing SAM, whereas Opi1p represses some of these genes in addition to genes whose products catalyze methyltransferase reactions of phospholipid biosynthesis. These results suggested that a *met4*Δ cell does not produce sufficient SAM for growth and a subsequent *opi1* mutation stimulates SAM production. Indeed, we found that adding SAM to the media or overexpressing the SAM synthetase gene allowed *met4*Δ cells to grow like wild-type cells. These results suggest that coordinated expression of the sulfur and phospholipid pathways contributes to optimal growth by ensuring that cells can maintain the considerable requirement for methylation in the biosynthesis of cell membrane phospholipids.

Strain background	*met4*Δ growth phenotype[a]	Reference
S288C	–	Mountain *et al.* (1993)
S288C	–	Fauchon *et al.* (2002)[b]
S288C	Inviable	Giaever *et al.* (2002)
S288C	Slow-growing	Snoek and Steensma (2006)
W303	–	Patton *et al.* (2000)
W303	–	Aranda and del Olmo (2004)[c]
W303	–	Leroy *et al.* (2006)[d]
W303	–	Lee *et al.* (2010)[d]
BF264-15D	–	Kaiser *et al.* (2000)[e]
CY4	–	Wheeler *et al.* (2002)[f]
4094-B	–	Masselot and De Robichon-Szulmajster (1975) [g]

[a]Phenotypes in the presence of exogenous methionine. –,no phenotype besides methionine auxotrophy.
[b]Strains in this study are made from the YPH98 strain, derived from YNN216, which is "congenic with S288C" (Sikorski and Hieter, 1989).
[c]This study used a *met4*Δ strain in the W303 background that was created and used in earlier studies (Thomas *et al.*, 1992; Kuras *et al.*, 1996).
[d]This study used a *met4*Δ strain in the W303 background that was created in an earlier study (Rouillon *et al.*, 2000).
[e]This study used the BF264-15D strain from Bruce Futcher (Reed *et al.*, 1985).
[f]This study used the CY4 strain first mentioned in a previous study (Grant *et al.*, 1996).
[g]This study used a methionine auxotroph that was isolated by UV mutagenesis. The identity of the mutation is not known.

TABLE 1: Strain backgrounds and phenotypes of *met4*Δ alleles.

RESULTS

Met4p is required for normal growth, even in the presence of excess exogenous methionine

A *met4*Δ strain is a methionine auxotroph (Masselot and De Robichon-Szulmajster, 1975) but has been reported to have varying phenotypes in rich media, such as yeast extract/peptone/dextrose (YPD), that contain the exogenous methionine required for growth (Table 1). We noticed that fresh *met4*Δ haploid transformants formed very small colonies on YPD plates, even when provided with additional methionine. This phenotype was unstable: plating after overnight growth in YPD produced a mixture of small and large colonies. We decided to investigate this phenomenon by transforming a *met4*Δ allele into a diploid strain. The *met4*Δ/*MET4* heterozygous diploid formed large colonies, similar to wild type, suggesting that a cell with one copy of *MET4* is not haploinsufficient. To test more rigorously the growth phenotype of *met4*Δ haploids, we sporulated this diploid and followed growth of the haploid spore colonies on YPD plates (Figure 1A). The *MET4* wild-type haploid grew as expected, but there was no *met4*Δ growth until day 3, suggesting that *MET4* is not absolutely essential for growth but is required for the optimal rate of growth. This growth defect always segregated 2:2 with the *met4*Δ allele, indicating that it was caused by loss of *MET4*.

We initially tested three obvious explanations for *met4*Δ slow growth and found that none of them accounted for the phenotype. First, this growth defect is not the result of abnormal germination, the process by which the spore transitions to mitotic cycling, because this slow-growth phenotype is maintained even when post-spore cells are streaked onto a fresh YPD plate (Figure 1A, bottom).

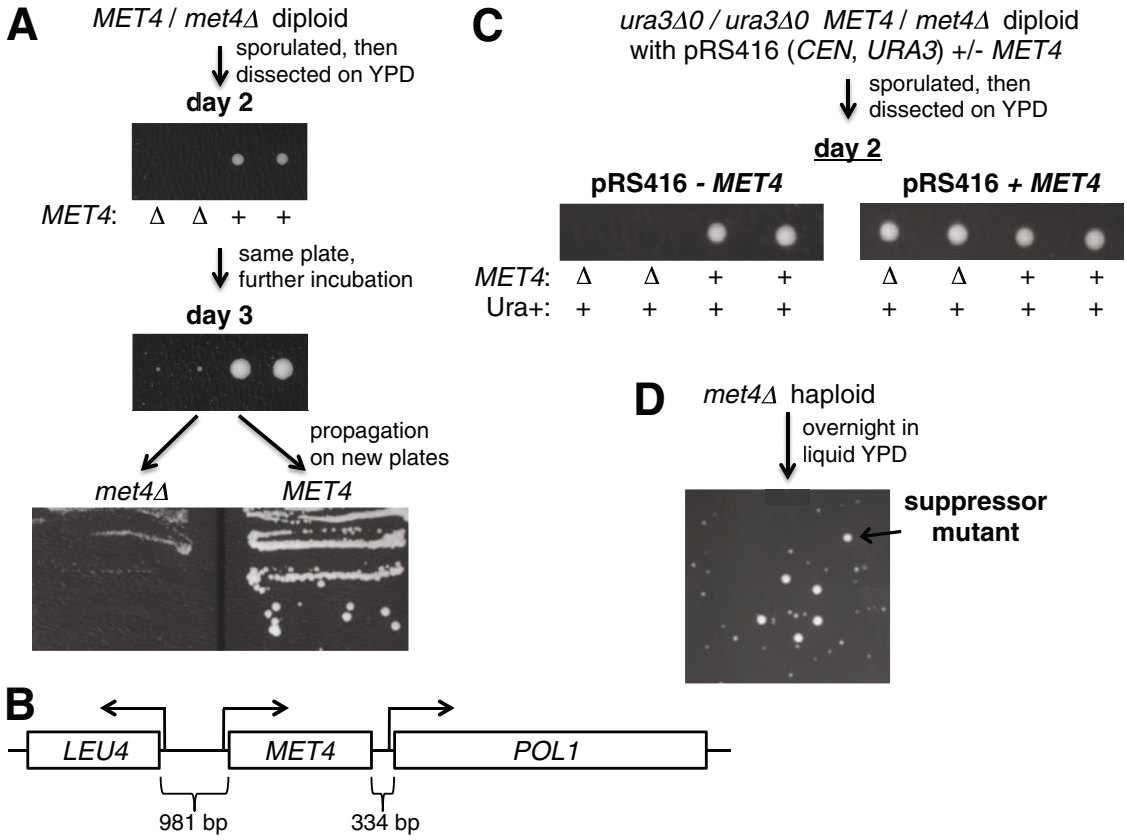

FIGURE 1: Deleting *MET4* causes slow growth, and this slow growth is spontaneously suppressed. (A) A *met4*Δ haploid grows poorly compared with *MET4*. A *met4*Δ/*MET4* heterozygote (DBY12042) was sporulated, and the resulting tetrads were dissected on YPD plates. To show that the growth defect was not a simply a germination defect and persisted over many divisions, the spore colonies were restreaked onto fresh YPD plates and grown for 2 d (bottom). A *MET4* wild type (FY4) is used as a control. Restreaking multiple times had the same effect. (B) The genomic locus surrounding the *MET4* ORF (denoted by a box), showing that expression of the essential *POL1* gene may be affected by deleting the *MET4* ORF. (C) The *met4*Δ growth defect can be rescued by a plasmid containing *MET4*. A *met4*Δ/*MET4* heterozygote containing either a *MET4* plasmid (DBY12210, right) or a control plasmid (DBY12211, left) was sporulated, and the resulting tetrads were dissected on YPD plates. (D) When *met4*Δ haploid cells (DBY12213) are grown overnight in liquid rich medium, fast-growing cells arise in the population. This was repeated with *met4*Δ cells from ~30 independent tetrads generated by sporulation of a *met4*Δ/*MET4* heterozygote, with very similar results.

Second, the poor growth of a *met4*Δ mutant was not due to insufficient import of exogenous methionine, because overexpression of the methionine transporters did not rescue this phenotype (Supplemental Figure S1). Third, the slow growth is not due to the absence of aerobic respiration, which requires sulfur metabolism (Bihlmaier *et al.*, 2007), because *met4*Δ can grow on a nonfermentable carbon source (glycerol/ethanol) (Supplemental Figure S2).

The *MET4* gene is only 334 base pairs upstream of the essential *POL1* gene (Figure 1B), so we were concerned that the slow growth of a *MET4*-deletion mutant actually resulted from a perturbation of *POL1*. To rule out this possibility, we complemented *met4*Δ with a plasmid containing only the *MET4* gene (Figure 1C). This plasmid did indeed allow *met4*Δ cells to grow like wild type, whereas a control plasmid lacking *MET4* had no effect on *met4*Δ slow growth. These results indicated that it was the loss of *MET4*, and not loss of *POL1* or other genes, that was responsible for the growth defect. The plasmid that we used contains the selectable gene *URA3*, so we attempted to select for loss of the plasmid by growing cells on 5-fluoroorotic acid (5-FOA), a drug that kills *URA3*-expressing cells. However, we found that *met4*Δ cells with a *MET4* plasmid did not grow at all on 5-FOA because *met4*Δ cells alone do not grow on 5-FOA, even after extended incubation periods (Supplemental Figure S3).

The growth defect of *met4*Δ can be spontaneously suppressed

When *met4*Δ cells from an overnight liquid culture in YPD are plated, they give rise to a mixture of small and large colonies (Figure 1D). The size of the small colonies is similar to that of the previously observed *met4*Δ colonies. The size of the larger colonies is similar to that of wild-type colonies, suggesting that the *met4*Δ growth phenotype has been effectively suppressed. This large size is maintained when cells from a large colony are streaked onto fresh YPD plates, indicating that large colony size is mitotically stable (Supplemental Figure S4A). These cells remain methionine auxotrophs, separating the role of Met4p in methionine biosynthesis from its role in controlling cell growth. In addition, we found that this suppression phenotype is meiotically inherited by a mutation in an unlinked gene (Supplemental Figure S4B). To show this, the suppressed *met4*Δ strain was crossed to a *MET4* strain and the resulting diploid was dissected. Half of the *met4*Δ spores produced small colonies and half produced wild type–sized colonies, as would be expected

if the suppression were the result of a mutation in a single gene unlinked to *MET4*.

Identifying mutations that suppress the growth defect of *met4*Δ

To identify the gene(s) in which suppressor mutations arise, we isolated such suppressors from 24 independent cultures, each of which was started by a *met4*Δ mutant (small colony) from tetrad dissection of a heterozygous diploid, as in Figure 1D. In each case, large colonies were present at a high frequency, and we selected one of these colonies from each independent culture for further analysis. We performed initial complementation testing and found that these 24 mutants fell into several complementation groups, suggesting that suppression can be caused by a mutation in any of several different genes. To find potential causative mutations, we hybridized genomic DNA from several *met4*Δ suppressor mutants and their parental *MET4* strains to whole-genome tiling arrays and then used a computer program (SNPScanner) (Gresham *et al.*, 2006) to compare the genome sequence of each mutant to its parent. In this way, we found single-nucleotide polymorphisms (SNPs) in one of three genes: *OPI1*, *TUP1*, or *DOT6*. Then we sequenced the entire *OPI1*, *TUP1*, and *DOT6* open reading frames in all 24 strains and found that nine strains contained potential mutations in *OPI1*, 2 had potential mutations in *TUP1*, and 1 had a potential mutation in *DOT6* (Table 2). Two additional strains (DBY12223 and DBY12222 in Table 3 later in the paper) have genomic rearrangements at *OPI1* that should produce an *opi1* loss-of-function mutant phenotype. Finally, there were 10 strains in which no mutations were observed, possibly because either 1) the strains contained *OPI1*, *TUP1*, or *DOT6* mutations (e.g., genomic rearrangements) that could not be detected by our analysis, or 2) the strains have mutations in other genes. Genetic analysis (see later discussion) confirmed that the *OPI1* and *TUP1* mutations are indeed causal; the *DOT6* SNP was not studied further.

Mutations in *TUP1* suppress the growth defect of *met4*Δ

Two SNPs in the *TUP1* open reading frame were found to potentially suppress the *met4*Δ growth defect (Table 2). These SNPs resulted in two amino acid changes that were very close together, as shown in the domain structure of the Tup1 protein (Figure 2A). Tup1 is a general transcriptional corepressor that represses many genes in yeast and is recruited to DNA by transcription factors (Malave and Dent, 2006). Of note, the mutations that we isolated specifically affect a surface of a WD40 propeller blade that interacts with MAT2 and possibly other transcription factors (Komachi and Johnson, 1997; Sprague *et al.*, 2000), suggesting that disruption of Tup1 binding to transcription factors like Opi1p (discussed later) might be responsible for *met4*Δ growth suppression. To test whether deleting *TUP1* suppresses the poor growth of *met4*Δ, we created a diploid strain that was heterozygous for both *met4*Δ and *tup1*Δ (Figure 2B). Then this diploid was sporulated and dissected on YPD plates, creating spores with all combinations of deletions. As has been widely observed, we found that a *tup1*Δ strain grew slower than did the wild type. Nonetheless, a *met4*Δ *tup1*Δ strain grew better than a *met4*Δ strain, indicating that *tup1*Δ suppresses the *met4*Δ growth defect.

Deleting *OPI1* suppresses the growth defect of *met4*Δ

The mutations in the *OPI1* gene (Table 2) were overlaid on the domain structure of the Opi1p protein (Figure 3A). This map shows that a variety of mutations, including severe mutations that prevent expression of the C-terminal two-thirds of Opi1p, potentially suppress the *met4*Δ growth defect. This suggested that loss of Opi1p

Nucleotide mutation[a]	Amino acid change
OPI1	
G376T[b]	E126amber
A409T	K137amber
G565T	E189amber
C614G	S205umber
A676G	K226E
T764C	L255S
C859T	Q287amber
C907T	Q303ochre
TUP1	
C2091G	S697R
G2095T	D699Y
DOT6	
C293A	S98amber

[a]Relative to beginning of open reading frame.
[b]Observed in two suppressor mutants.

TABLE 2: Identity of the *met4*Δ suppressor mutations.

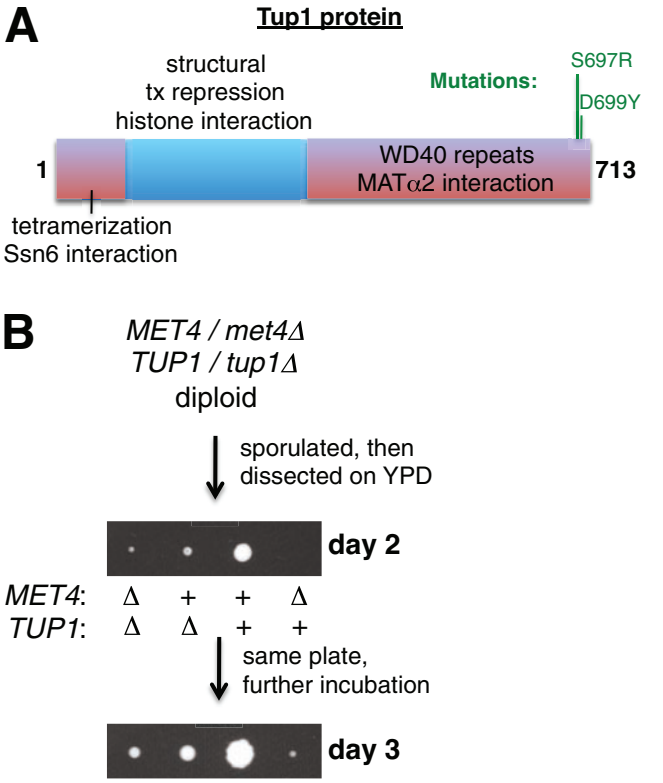

FIGURE 2: Mutations in *TUP1* suppress the growth defect of *met4*Δ. (A) We found two *met4*Δ-suppressed strains with mutations in the *TUP1* gene (Table 2). The mutations (S697R and D699Y) are depicted in relation to the encoded Tup1p protein and its previously determined domains (Komachi and Johnson, 1997), and they are in a region of the protein that affects Tup1p interaction with transcription factors (Sprague *et al.*, 2000). (B) Deletion of *TUP1* causes a *met4*Δ haploid to grow significantly better. A *met4*Δ/*MET4 tup1*Δ/*TUP1* diploid (DBY12232) was sporulated, and the resulting tetrads were dissected on YPD plates. The *met4*Δ *tup1*Δ cells remained methionine auxotrophs.

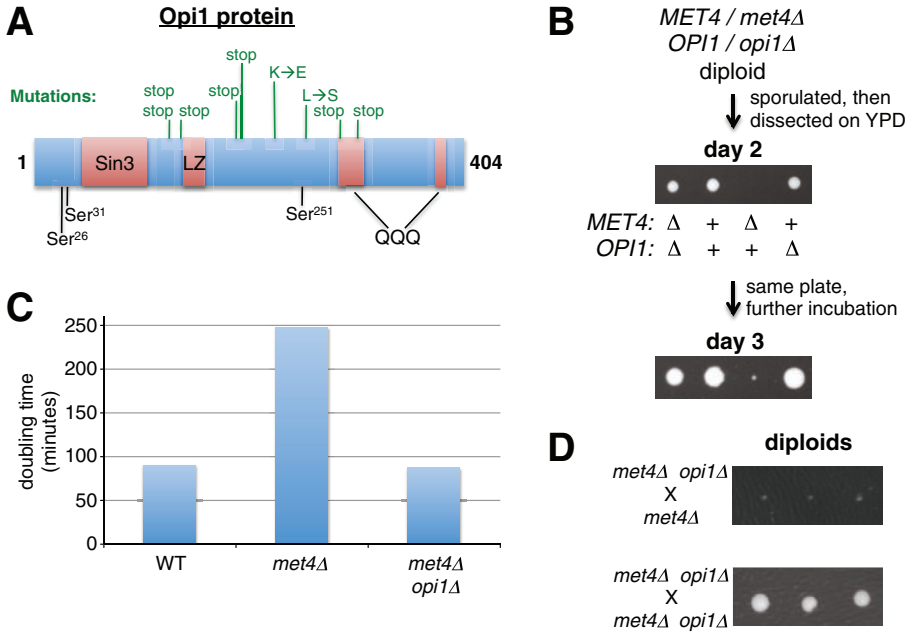

FIGURE 3: Opi1p is required for the slow growth of *met4*Δ cells. (A) The mutations in the *OPI1* gene are depicted in relation to the encoded Opi1p protein and its previously determined domains (Sreenivas and Carman, 2003). The following structural and functional domains are depicted: Sin3 (Sin3-interacting), LZ (leucine zipper), and QQQ (glutamine rich). Protein kinase A phosphorylates residues Ser-31 and Ser-251, whereas protein kinase C phosphorylates Ser-26. (B) Deletion of *OPI1* causes a *met4*Δ haploid to grow like wild type. A *met4*Δ/*MET4 opi1*Δ/*OPI1* diploid (DBY12225) was sporulated, and the resulting tetrads were dissected on YPD plates. The tetrads showed the 2:2, 3:1, and 4:0 large:small patterns as expected. The *met4*Δ *opi1*Δ cells remained methionine auxotrophs. (C) The doubling time of *met4*Δ is higher than that for *MET4* or *met4*Δ *opi1*Δ. The *MET4* (DBY12000), *met4*Δ (DBY12214), and *met4*Δ *opi1*Δ (DBY12226) strains were inoculated into YPD at low density and the cell concentration was followed until they reached saturation. The exponential phase of growth was used to calculate the doubling time only for cultures that did not develop growth suppression. A representative graph from many experiments is shown. (D) The *opi1*Δ allele acts recessively to suppress the growth defect of a *met4*Δ strain. Top, a *met4*Δ haploid (DBY12214) was crossed to a *met4*Δ *opi1*Δ haploid (DBY12227), and the resulting *met4*Δ/*met4*Δ *opi1*Δ/*OPI1* diploids (three are shown) were grown for 2 d. Bottom, a *met4*Δ *opi1*Δ haploid (DBY12227) was crossed to a *met4*Δ *opi1*Δ haploid (DBY12226), and the resulting *met4*Δ/*met4*Δ *opi1*Δ/*opi1*Δ diploids (three are shown) were grown for 2 d.

function may suppress the *met4*Δ phenotype and led us to test whether an *opi1*Δ allele deletion also suppresses the *met4*Δ phenotype. First, we created a diploid strain that was heterozygous for both *opi1*Δ and *met4*Δ (Figure 3B). Then this diploid was sporulated and dissected on YPD plates, creating spores with all combinations of deletions. As expected, we observed that *opi1*Δ suppressed the *met4*Δ growth defect. As a control, *opi1*Δ did not affect growth of an otherwise wild-type strain. To quantify the effect of *OPI1* on growth rate, we compared the doubling times of these strains in liquid YPD, which confirmed that *met4*Δ grows more slowly (i.e., has a greater doubling time) than either *MET4* or *met4*Δ *opi1*Δ (Figure 3C). The *opi1*Δ allele acted recessively, as expected, because crossing a *met4*Δ *opi1*Δ strain to a *met4*Δ strain resulted in slow-growing diploids (Figure 3D, top). As a control, crossing a *met4*Δ *opi1*Δ strain to a *met4*Δ *opi1*Δ strain resulted in normally growing diploids (Figure 3D, bottom).

Simultaneously studying transcriptional regulation by Met4p and Opi1p

We further investigated the genetic interaction between Opi1p and Met4p because, in addition to the results presented earlier, we previously found that the expression of two Opi1p targets (*OPI3* and *CKI1*) depends specifically on methionine and sulfur abundance (Petti *et al.*, 2011). Given that both Opi1p and Met4p are transcriptional regulators, we sought to understand their genetic interaction from a transcriptional perspective. Because a *met4*Δ strain readily develops growth suppressor mutations, we studied Met4p transcriptional regulation using a system in which Met4p can be quickly degraded by an estradiol-inducible TEV protease (McIsaac *et al.*, 2011). Such a system is indispensable for studying unstable deletion phenotypes like that of *met4*Δ, because the target protein (in this case, Met4p) is degraded with a half-life of ~15 min, well before suppressor mutations can arise. We used the *NDeg-MET4* strain containing the machinery necessary for estradiol induction, an inducible TEV protease gene, and the *MET4* gene N-terminally tagged with a TEV protease site. To simultaneously study Opi1p transcriptional regulation, we used a pair of strains: 1) *NDeg-MET4*, in which *OPI1* is wild type, and 2) *opi1*Δ *NDeg-MET4*. We also included a control strain that contains the estradiol-induction machinery and inducible TEV protease gene but wild-type *MET4* and *OPI1* genes.

To compare gene expression across these strains, we grew each to midexponential phase in minimal medium, added estradiol, and measured mRNA abundance at several time points up to 6 h after estradiol addition (Supplemental Data Set S1). We focused our analysis on the immediate response observed within 30 min after estradiol addition (*Materials and Methods*). Confirming that Met4p is degraded, we found that the canonical Met4p targets (Lee *et al.*, 2010) are indeed turned off after estradiol addition (Figure 4). Many of these targets are slightly turned off in the control strain, but they are significantly more turned off in the *NDeg-MET4* strain (see Figure 5 and Supplemental Data Set S1). Furthermore, many of the targets known to be repressed by Opi1p (Santiago and Mamoun, 2003) are derepressed in *opi1*Δ *NDeg-MET4* compared with *NDeg-MET4* (Figure 4).

In an initial, semiquantitative comparison of *NDeg-MET4* and *opi1*Δ *NDeg-MET4*, we found that *INO1* exhibited the most striking difference between the strains (Figures 4 and 5B). *INO1*, a gene required for inositol biosynthesis, is the best-described target of Opi1p (White *et al.*, 1991). It is also a target of Cbf1, a DNA-binding partner of Met4p (Shetty and Lopes, 2010). Even before estradiol addition, the *INO1* transcript is ~32 times more abundant in *opi1*Δ *NDeg-MET4* than in the other strains. *INO1* expression increases over time in all three strains (including the control), reaching a final abundance in *opi1*Δ *NDeg-MET4* that is 23 times greater than in *NDeg-MET4* and 9 times greater than in the control.

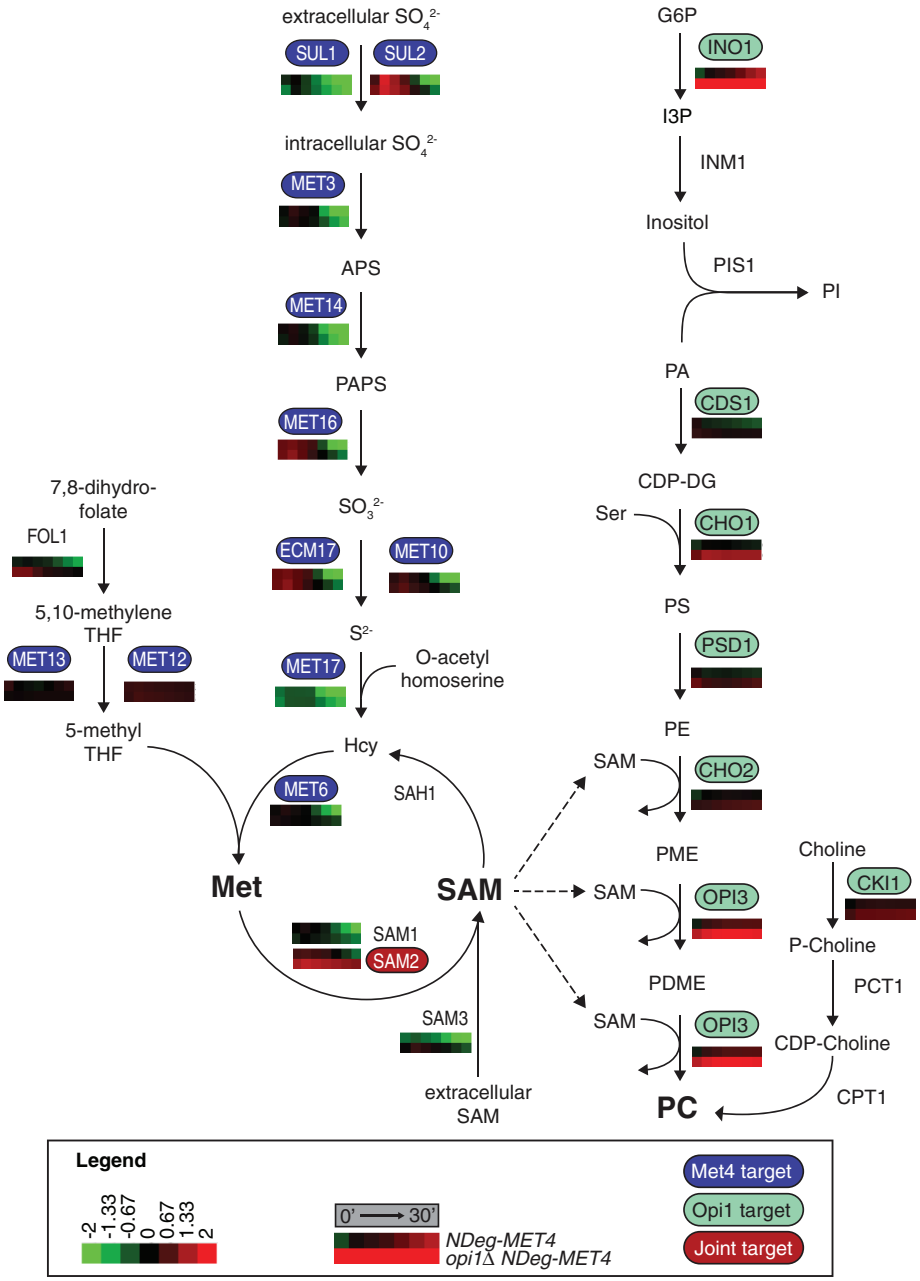

FIGURE 4: Role of Met4p and Opi1p in regulating sulfur assimilation and PC biosynthesis pathways. Gene expression data for the biosynthesis genes were overlaid on the pathways. Gene expression time courses for a given gene are shown beneath that gene. Top and bottom, *NDeg-MET4* and *opi1Δ NDeg-MET4*, respectively, with $\log_2$ fold change as indicated in the legend. Gene expression time courses are displayed as in the legend: from the instant before 1 μM estradiol treatment (0′) until 30 min after treatment (30′). Values at 0, 5, 15, and 30 min represent actual experimental measurements (indicated with black boxes above the time course), whereas values at 10, 20, and 25 min represent interpolated values (indicated with gray boxes above the time course) (see *Materials and Methods*). Genes directly regulated by Met4p (Lee *et al.*, 2010) are shown in blue; genes directly regulated by Opi1p (Santiago and Mamoun, 2003) are shown in green; joint targets are shown in red. CDP-choline, cytidine diphosphate choline; CDP-DG, cytidine diphosphate diacylglycerol; APS, 5′-adenylylsulfate; G6P, glucose 6-phosphate; Hcy, homocysteine; I3P, inositol 3-phosphate; Met, methionine; P-choline, phosphocholine; PA, phosphatidic acid; PAPS, 3′-phospho-5′adenylylsulfate; PC, phosphatidylcholine; PDME, phosphatidyl-dimethylethanolamine; PE, phosphatidylethanolamine; PI, phosphatidylinositol; PME, phosphatidyl-monomethyl-ethanolamine; PS, phosphatidylserine; S^{2-}, sulfide; SAM, *S*-adenosylmethionine; SO_3^{2-}, sulfite; SO_4^{2-}, sulfate; THF, tetrahydrofolate.

Deleting or manipulating expression of *INO1* has no effect on the growth of either *met4Δ* or *met4Δ opi1Δ* strains

To test whether the slow growth phenotype of *met4Δ* is due to *INO1* misregulation, we made a *met4Δ/MET4 GAL1*$_{pr}$*-INO1/INO1* diploid strain, sporulated it and dissected the spores on yeast extract/peptone (YP) media either with glucose or galactose as a carbon source (to turn off or on *INO1* expression, respectively). We found that repression or overexpression of *INO1* had no effect on *met4Δ* growth (Supplemental Figure S5A). Next we wanted to know whether the normal growth of *met4Δ opi1Δ* was due to a change in *INO1* expression. We therefore made a *met4Δ/MET4 opi1Δ/OPI1 ino1Δ/INO1* diploid strain, sporulated it, and dissected the spores on YPD media. Deleting *INO1* had no effect on the growth of any strains, including a *met4Δ* mutant and a *met4Δ opi1Δ* mutant (Supplemental Figure S5B). These data show that *INO1* is not involved in the regulation of growth by Met4p and Opi1p.

Gene expression analysis suggests that Met4p and Opi1p both regulate SAM levels

Next we searched for other gene expression differences that might explain the role of Met4p and Opi1p in growth regulation. We began by using multiple regression to quantify the dependence of each gene in the original data set on Met4p and Opi1p (see *Materials and Methods* for data processing and filtering). This analysis identified most of the known Met4p and Opi1p target genes (Santiago and Mamoun, 2003; Lee *et al.*, 2010), as well as other genes that may either be indirectly regulated or newly identified targets (Figure 5). All of these genes can be grouped into three categories: 1) 75 genes affected only by Met4p abundance (Figure 5A), 2) 65 genes affected only by Opi1p abundance (Figure 5B), and 3) 43 genes affected by both Met4p and Opi1p (Figure 5C). This coregulation by Met4p and Opi1p is statistically significant ($p < 0.0001$), suggesting that the biochemical processes regulated by Met4p (sulfur assimilation) and Opi1p (phospholipid biosynthesis) are interdependent. However, almost all coregulation by Met4p and Opi1p is carried out by indirect or nontranscriptional mechanisms, because only one gene, *SAM2*, has been shown to be regulated by both Met4p and Opi1p (Santiago and Mamoun, 2003; Lee *et al.*, 2010). The *SAM2* gene will be discussed later.

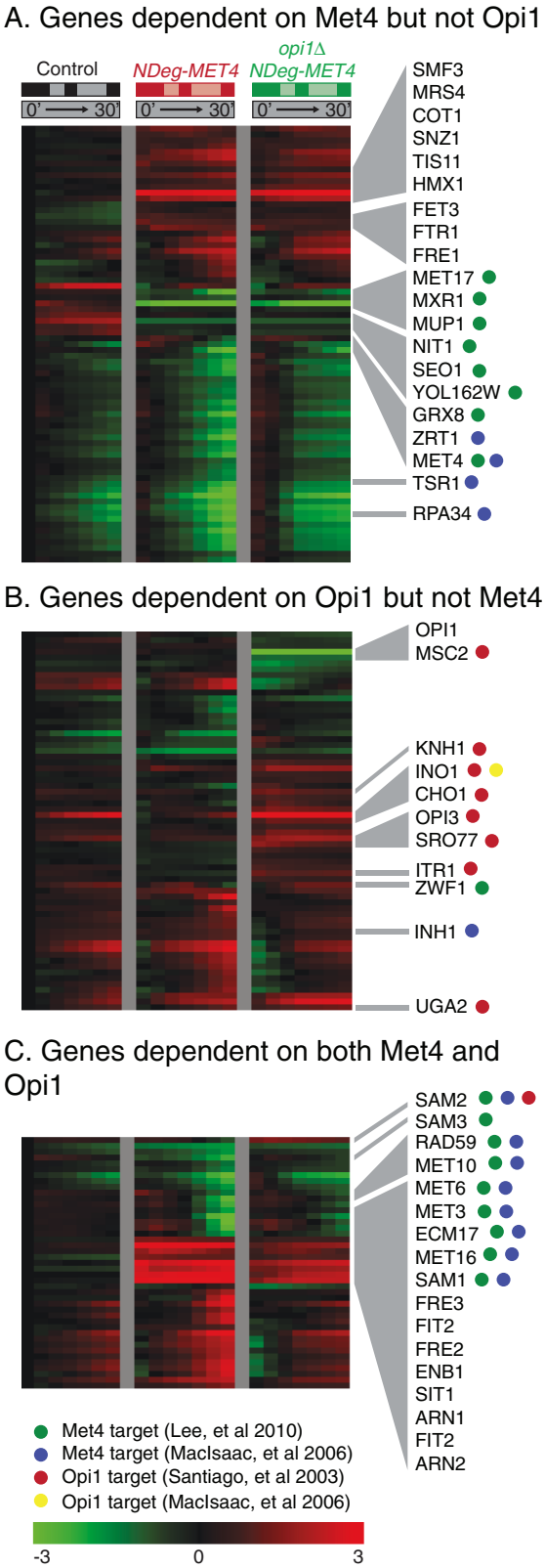

FIGURE 5: Genome-wide expression analysis of Met4p and Opi1p regulation. Multiple regression was used to identify genes whose expression is primarily dependent on Met4p abundance (A), Opi1p abundance (B), or both (C). Three strains (the control strain, *NDeg-MET4*, and *opi1Δ NDeg-MET4*) were treated with 1 μM estradiol. Gene expression is shown from the instant before estradiol treatment (0′) until 30 min after treatment (30′), with $\log_2$ fold change as indicated in the legend. Values at 0, 5, 15, and 30 min represent actual experimental measurements (indicated with black, red, or dark green boxes above the time courses, respectively), whereas values at 10, 20, and 25 min represent interpolated values (indicated with gray, pink, or light green boxes above the time courses, respectively; see *Materials and Methods*). Only genes that change by a factor of at least 1.5 in at least one time course are shown. Gene names discussed in the text are shown in the figure. Previously identified targets of Met4p are indicated with green (Lee *et al.*, 2010) or blue (MacIsaac *et al.*, 2006). Previously identified targets of Opi1p are indicated with red (Santiago and Mamoun, 2003) or yellow (MacIsaac *et al.*, 2006) dots.

To further understand how Opi1p specifically affects growth of a *met4Δ* strain, we analyzed the 108 genes that are Opi1p regulated (i.e., differentially expressed between *opi1Δ NDeg-MET4* and *NDeg-MET4*; false-discovery rate [FDR] < 0.1; Figure 5, B and C). This set is highly enriched for genes whose products 1) associate with the cellular membrane and 2) function in cation homeostasis, oxidation–reduction, sulfur assimilation, the trichloracetic acid cycle, carbohydrate metabolism, and transmembrane transport (Supplemental Data Set S2). Notably, this set also contains three of the five genes that regulate intracellular SAM abundance: the two SAM synthetase genes (*SAM1* and *SAM2*) and the SAM transporter gene (*SAM3*; p = 0.0016 by hypergeometric distribution). From this analysis, we speculated that deleting *OPI1* suppresses the growth defect of a *met4Δ* strain by affecting one or more of these Opi1p-regulated processes.

Inspection of the metabolic pathways governing phospholipid biosynthesis reveals that PC biosynthesis, which is repressed by Opi1p, requires SAM at three steps (Figure 4; Chin and Bloch, 1988). We overlaid gene expression data on the metabolic pathways regulated by Met4p and Opi1p and found that several SAM biosynthesis genes are activated by Met4p and repressed by Opi1p. Most notably, *SAM2* is weakly activated by Met4 and strongly repressed by Opi1 ($p = 9.4 \times 10^{-3}$ based on use of the F test to compare *opi1Δ NDeg-MET4* and *NDeg-MET4*; see *Materials and Methods*). Average *SAM2* abundance, which changes little in response to estradiol, is 5.5 times higher in *opi1Δ NDeg-MET4* than in *NDeg-MET4* (p = 0.038 by Student's *t* test). *SAM3* behaves similarly (p = 0.003 by the F test); on average, *SAM3* abundance is 12 times higher in *opi1Δ NDeg-MET4* than in *NDeg-MET4* (p = 0.078 by Student's *t* test). Although *SAM1* follows a similar pattern, it is only weakly repressed by *OPI1*: during the first 30 min after estradiol addition, *SAM1* abundance falls nearly fourfold in *NDeg-MET4* and 2.1-fold in *opi1Δ NDeg-MET4*. Thus the interdependence of Met4p- and Opi1p-regulated pathways may be based on SAM metabolism. In previous work, we found that SAM is rapidly and dramatically depleted in methionine auxotrophs (Petti *et al.*, 2011). We therefore hypothesized that *met4Δ* mutants grow slowly because they lack sufficient SAM for PC biosynthesis.

Increased amounts of SAM suppress the growth defect of *met4Δ*

SAM is required for growth and can be either synthesized endogenously by Sam1p or Sam2p or added exogenously to a SAM auxotroph. However, SAM is not present in YPD because it is a highly unstable metabolite and thus likely does not survive the autoclaving process (Kuras *et al.*, 2002). Therefore we predicted that *met4Δ* cells grow slowly because they are unable to express the Met4p-regulated *SAM2* gene and thus synthesize SAM. To test this, we first sporulated a *met4Δ/MET4* heterozygote and dissected the spores on YPD with freshly added SAM (Figure 6A). Indeed, we found that a *met4Δ* spore grew almost as well as a wild-type spore under these

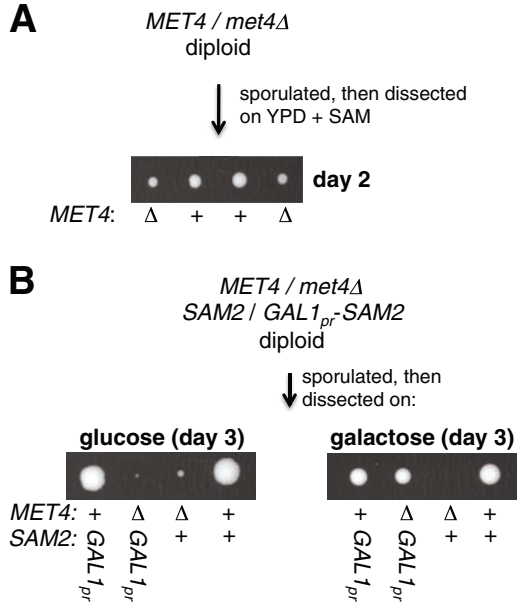

FIGURE 6: Increasing intracellular levels of SAM suppresses the growth defect of *met4*Δ. (A) Adding SAM to YPD rescues growth of a *met4*Δ haploid. A *met4*Δ/*MET4* heterozygote (DBY12043) was sporulated, and the resulting tetrads were dissected on YPD plates with 0.2 mM SAM. Many SAM concentrations (0.05–0.5 mM) were tested, with 0.2 mM supporting the optimal *met4*Δ growth. The *met4*Δ cells remained, as expected, methionine auxotrophs. (B) Overexpression of the *SAM2* gene rescues growth of a *met4*Δ haploid. A *met4*Δ/*MET4 GAL1*$_{pr}$-SAM2/*SAM2* heterozygote (DBY12233) was sporulated, and the resulting tetrads were dissected on YPD or YPGal plates.

conditions. Next we created a *met4*Δ/*MET4 GAL1*$_{pr}$-*SAM2*/*SAM2* diploid strain, sporulated it, and dissected spores on YP media either with glucose or galactose as a carbon source (to turn off or on *SAM2* expression, respectively) (Figure 6B). As expected, a *met4*Δ *GAL1*$_{pr}$-*SAM2* spore grew like wild type on galactose (when overexpressing *SAM2*) and poorly on glucose (with *SAM2* turned off). Thus the poor growth of *met4*Δ cells can be suppressed by increasing the intracellular concentration of SAM.

Expression data suggest that Met4p and Opi1p both indirectly affect membrane function

The Met4p-dependent genes that we identified earlier have a wide variety of cellular functions (Supplemental Data Set S2). One group of genes, those repressed by Met4p (i.e., induced during Met4p degradation), is enriched for iron homeostasis genes (*FTR1, SMF3, COT1, MRS4, FET3, FRE1*; Figure 5A; FDR < 0.1). These genes were derepressed even before estradiol was added to the *NDeg-MET4* strain, suggesting that Met4p may be slightly unstable in this strain due to modification and that these genes are very sensitive to the levels of Met4p. Consistent with these data, we previously observed dramatic induction of the same iron homeostasis genes upon deletion of *MET31* and *MET32* (Petti *et al.*, 2011).

We found that these and additional iron homeostasis genes *(FRE3, FRE2, FIT2, SIT1, ARN1, FIT3, MSC2, ARN2, ENB1*) are also activated by Opi1p (i.e., less strongly induced by Met4p degradation in *opi1*Δ *NDeg-MET4* than in *NDeg-MET4*; Figure 5C). Surprisingly, none of these genes is a known direct target of Met4p or Opi1p (or Met31/Met32/Cbf1; Figure 5, A–C), indicating that Met4p and Opi1p affect iron homeostasis by indirect regulation of expression. Of note, all of the proteins encoded by these genes are physically located in or at the cellular membrane, suggesting the following hypothetical chain of regulatory events: Met4p degradation leads to a drop in SAM levels and a subsequent decrease in PC biosynthesis. This PC decrease perturbs a wide variety of processes, such as iron homeostasis, that depend on cellular membranes for transport and intracellular homeostasis. Deleting *OPI1* bypasses the decrease in PC biosynthesis, alleviating the perturbation in iron homeostasis.

The *met4*Δ slow-growth phenotype occurs in the W303 strain background

We found that deleting *MET4* in the S288C genetic background causes slow growth. We wanted to test whether this is the case in another background, W303, which has been used extensively in studying Met4p (Table 1). We found that two previously generated *met4*Δ strains have frameshift *opi1* mutations that allow them to grow normally. On crossing these strains to a wild-type strain and sporulating the diploid, we found that half of the resulting *met4*Δ spores grew slowly (no suppression) and the other half grew normally (suppressed). The *met4*Δ slow growth can be rescued by adding SAM to the media (Supplemental Figure S6).

DISCUSSION

Met4p has long been known to regulate the genes of the sulfur assimilation pathway, which is responsible for the incorporation of extracellular sulfate into methionine, cysteine, homocysteine, and SAM. Indeed, Met4p was previously shown to be required for methionine biosynthesis (Masselot and De Robichon-Szulmajster, 1975). We show here that Met4p also contributes to the biosynthesis of SAM, an essential metabolite that serves as the methyl donor in most methyltransferase reactions (Thomas and Surdin-Kerjan, 1997). Specifically, we found that SAM must be added to YPD in order for *met4*Δ cells to grow at wild-type rates, indicating that *met4*Δ is not only a methionine auxotroph but also a partial SAM auxotroph even in the presence of excess methionine, either provided in the medium or by overexpression of a methionine transporter. However, *met4*Δ cells are able to grow, albeit slowly, on YPD, indicating that *met4*Δ cells either carry out limited SAM biosynthesis from methionine or import some SAM from rich media.

The increased SAM requirement of *met4*Δ is consistent with the known role of Met4p in regulating the expression of genes required for SAM biosynthesis, specifically the biosynthetic *MET* and *SAM* genes (Thomas and Surdin-Kerjan, 1987; Thomas *et al.*, 1988; Rouillon *et al.*, 2000; Lee *et al.*, 2010). These genes are directly induced by Met4p (Lee *et al.*, 2010), consistent with our microarray analysis showing that expression of these genes decreases upon Met4p degradation (Figures 4 and 5 and Supplemental Data Set S1). In addition, Met4p degradation decreases the expression of *FOL1*, encoding an enzyme in the folate metabolism pathway that contributes a methyl group in the conversion of homocysteine to methionine.

The *met4*Δ growth defect can be suppressed by increasing endogenous SAM levels, as described earlier, or by spontaneous loss-of-function mutations in a variety of genes, including *OPI1* and *TUP1*. Independently deleting *OPI1* or *TUP1* in a *met4*Δ strain recapitulated the effects of these mutations. Our expression microarray analysis showed that Opi1p represses *SAM2* expression, whereas Met4p induces *SAM2*, consistent with previous results (Kodaki *et al.*, 2003; Santiago and Mamoun, 2003; Jesch *et al.*, 2005). This suggests that *opi1*Δ suppresses *met4*Δ slow growth by derepressing *SAM2* and thereby increasing SAM levels. Indeed, overexpression of *SAM2* is sufficient to suppress the growth defect of a *met4*Δ strain. The ability of a *tup1*Δ allele to suppress the *met4*Δ growth defect may also lie in its ability to compensate for the SAM deficiency of *met4*Δ. This is

because Tup1, like Opi1p, represses *SAM2*, as Tup1 is required for repression of Opi1p-regulated genes (Wagner *et al.*, 2001).

Our experiments suggest that derepression of *SAM2* is the main mechanism of suppressing the *met4*Δ growth defect, but Opi1p inactivation might compensate for the SAM deficiency through four alternative mechanisms. First, an *opi1* mutation derepresses all of the PC biosynthetic genes (*CDS1*, *CHO1*, *PSD1*, *CHO2*, and *OPI3*), thereby increasing flux through the pathway. If PC is the major consumer of SAM, as we argue later, this may allow cells to produce sufficient PC when SAM levels are low. Second, an *opi1* mutation derepresses expression of *CKI1*, required for the Kennedy pathway that produces PC without SAM. However, this pathway uses choline obtained from the breakdown of PC and thus cannot be used for de novo PC biosynthesis. Third, an *opi1* mutation derepresses methionine biosynthetic genes, presumably leading to increased production of methionine and SAM. Fourth, an *opi1* mutation derepresses the *FOL1* gene, a component of the folate cycle that donates a methyl group for methionine biosynthesis. The result could be increased levels of methionine and subsequently SAM.

Our results point to transcriptional and metabolic coordination between the sulfur assimilation pathway, regulated by Met4p, and the PC biosynthetic pathway, regulated by Opi1p. Previous work implied that these pathways are connected through SAM-dependent methylation (Santiago and Mamoun, 2003; Malanovic *et al.*, 2008; Petti *et al.*, 2011). Here we show that Opi1p and Met4p genetically interact because they both contribute to regulating SAM levels. The sulfur assimilation pathway is required for the biosynthesis of SAM, which provides a methyl group during three steps in PC biosynthesis (Figure 4). Opi1p directly represses *SAM2* expression as well as PC biosynthetic genes, likely to maintain coordination of SAM levels with the SAM requirement of PC biosynthesis. Our search of the *SAM2* literature and for potential binding sites in the *SAM2* promoter shows that, besides the Met4p transcriptional complex, Opi1p is the only known direct regulator of *SAM2*. From this finding, we hypothesize that PC biosynthesis accounts for the majority of SAM-dependent methylation reactions, although this remains to be tested. Phospholipids represent a major portion of the dry weight of a yeast cell (Nurminen *et al.*, 1976; Strathern *et al.*, 1982), with PC making up at least 30% of phospholipids (Strathern *et al.*, 1982). As shown in Figure 4, PC is biosynthesized de novo from another phospholipid, phosphatidylethanolamine (PE), in three SAM-consuming methyltransferase reactions catalyzed by Opi3 and Cho2 (Chin and Bloch, 1988; Summers *et al.*, 1988; McGraw and Henry, 1989; Kodaki *et al.*, 2003). In contrast, ergosterol, another membrane lipid synthesized by SAM-dependent methylation, may be as abundant as PC (Nurminen *et al.*, 1976), but the synthesis of one ergosterol molecule only consumes one SAM (McCammon *et al.*, 1984). Thus the SAM requirement is three times higher to make PC than to make ergosterol. Although SAM is used in several other reactions, such as during the biosynthesis of biotin and polyamine and in the modification of RNA and proteins (Thomas and Surdin-Kerjan, 1997), these reactions are likely not significant consumers of SAM because the products are at relatively low levels in comparison to the membrane lipids.

OPI1 inactivation was the most common spontaneous mutation causing *met4*Δ suppression. We found that the mechanism of suppression is consistent with an increase in SAM levels, and *OPI1* inactivation is likely the simplest way to achieve this. Opi1p represses transcription by inhibiting the transcriptional activators Ino2 and Ino4, and therefore an *opi1*Δ mutant causes relative activation of Ino2/Ino4–dependent genes like *SAM2* (Santiago and Mamoun, 2003; Jesch *et al.*, 2005; Chen *et al.*, 2007). Because it is more likely that a mutation causes a loss of function (LOF) than a gain of function (GOF), increased *SAM2* expression is more likely to be caused by LOF *opi1* mutations than GOF mutations in *INO2*, *INO4*, the *SAM2* promoter, or other positive regulatory genes. There are other *SAM2* negative regulators, such as *TUP1*, that could be the target of LOF mutations. However, since *TUP1* itself is required for normal growth, few mutations in this gene will cause suppression without affecting growth. Indeed, the two *tup1* SNPs that we identified likely were this type of mutation because they were close together on the *TUP1* gene and resulted in growth that was better than that with *tup1*Δ.

Finally, our findings may be of clinical importance. It was previously shown that inhibiting the methylation steps of de novo PC biosynthesis, through deletion of *SAH1*, *OPI3*, or *CHO2*, leads to triacylglycerol accumulation, an indicator of several diseases, including heart disease (Malanovic *et al.*, 2008). We found that SAM deficiency caused by *met4*Δ may also inhibit the PC pathway. Our work shows that inactivation of Opi1p might prevent this inhibition and the consequent accumulation of triacylglycerol. Although humans do not have an Opi1p orthologue, they may have a similar mechanism for sensing phospholipid levels (Loewen and Levine, 2005). Thus targeting this mechanism could be a way to treat diseases of lipid accumulation. More generally, a more complete understanding of the regulatory relationships between metabolic pathways will be useful in understanding the etiology of metabolic diseases.

MATERIALS AND METHODS

Strains

All *S. cerevisiae* strains are listed in Table 3, and almost all are isogenic with a *GAL2*$^{+}$ derivative of S288C containing a repaired *HAP1* allele (Winston *et al.*, 1995; Hickman and Winston, 2007). The rest of the strains are in the W303 background. Strains were constructed by standard methods, either by crosses or by transformation (Ausubel, 2001). The deletion alleles were created by replacing the respective open reading frame (ORF) with the *KanMX* or *NatMX* (Brachmann *et al.*, 1998) or HphMX4 markers (Carter and Delneri, 2010). The *KanMX::GAL1*$_{pr}$*-ORF* alleles (where *ORF* = *SAM2*, *MUP1*, *MUP3*, or *INO1*) was constructed by placing the *KanMX* marker and the *GAL1* promoter upstream of the respective ORF (Longtine *et al.*, 1998). The selection drugs used were ClonNat (100 µg/ml; Werner BioAgents, Jena, Germany), G418 (100 µg/ml; Cellgro, Manassas, VA), and hygromycin (2900 U/ml; Calbiochem, La Jolla, CA).

Media and growth conditions

Cells were grown at 30°C in 1% yeast extract, 2% peptone, 2% glucose (YPD), unless otherwise noted. Yeast extract/peptone/galactose (YPGal) and YP + glycerol/ethanol contained 2% galactose and 2% of a 50/50 glycerol/ethanol mixture, respectively, in place of glucose. SAM (A7007; Sigma-Aldrich, St. Louis, MO) was made up in water at 20 mg/ml, filter sterilized, and added to YPD plates 1 d before plating cells. The *met4*Δ allele was maintained in a *met4*Δ/*MET4* heterozygous diploid to prevent suppressor formation; there was no haploinsufficiency or suppressor formation seen in this diploid. To create a *met4*Δ haploid with or without other mutations, the relevant diploid was sporulated by growing it to mid-log in YPD, washed in water, and grown in sporulation media (1% potassium acetate) for 3 d at room temperature. The resulting tetrads were dissected by dissection microscopy. As denoted in the figures, pictures were taken after 2 or more days of growth. In the figures, a representative tetrad may be shown, but at least 10 complete tetrads were analyzed for each diploid. The resulting spores were tested for all of the relevant marker phenotypes. All experiments in

Name	Genotype	Reference
FY4	MATa	Winston *et al.* (1995)
FY5	MATα	Winston *et al.* (1995)
DBY11250	MATa/α	This study
DBY12000	MATa *HAP1*$^{+}$	Hickman and Winston (2007)
DBY12001	MATα *HAP1*$^{+}$	Hickman and Winston (2007)
DBY12007	MATa/α *HAP1*$^{+}$/*HAP1*$^{+}$	Hickman and Winston (2007)
DBY12042	MATa/α *HAP1*$^{+}$/*HAP1*$^{+}$ *met4*Δ::KanMX/*MET4*	This study
DBY12043	MATa/α *HAP1*$^{+}$/*HAP1*$^{+}$ *met4*Δ::NatMX/*MET4*	This study
DBY12210	MATa/α *HAP1*$^{+}$/*HAP1*$^{+}$ *ura3*Δ*0/ura3*Δ*0 met4*Δ*::KanMX/MET4* pRS416+*MET4*	This study
DBY12211	MATa/α *HAP1*$^{+}$/*HAP1*$^{+}$ *ura3*Δ*0/ura3*Δ*0 met4*Δ*::KanMX/MET4* pRS416	This study
DBY12212	MATa/α *HAP1*$^{+}$/*HAP1*$^{+}$ *ura3*Δ*0/ura3*Δ*0 met4*Δ*::KanMX/MET4*	This study
DBY12213	MATa *HAP1*$^{+}$ *met4*Δ::KanMX	This study
DBY12214	MATa *HAP1*$^{+}$ *met4*Δ::NatMX	This study
DBY12215	MATa *HAP1*$^{+}$ *met4*Δ::KanMX *opi1-G376T*[a]	This study
DBY12216	MATa *HAP1*$^{+}$ *met4*Δ::NatMX *opi1-A409T*[a]	This study
DBY12217	MATa *HAP1*$^{+}$ *met4*Δ::KanMX *opi1-G565T*[a]	This study
DBY11402	MAT? *hap1*$^{-}$ *met4*Δ::NatMX *opi1-C614G*[a]	This study
DBY12218	MATa *HAP1*$^{+}$ *met4*Δ::KanMX *opi1-A676G*[a]	This study
DBY12219	MATα *HAP1*$^{+}$ *met4*Δ::NatMX *opi1-T764C*[a]	This study
DBY12220	MATa *HAP1*$^{+}$ *met4*Δ::NatMX *opi1-C859T*[a]	This study
DBY12221	MATa *HAP1*$^{+}$ *met4*Δ::NatMX *opi1-C907T*[a]	This study
DBY12222	MAT *HAP1*$^{+}$ *met4*Δ::NatMX *opi1*[b]	This study
DBY12223	MAT *HAP1*$^{+}$ *met4*Δ::KanMX *opi1*[b]	This study
DBY12224	MATa *HAP1*$^{+}$ *met4*Δ::NatMX *tup1-C2091G*[a]	This study
DBY11405	MATa *hap1*$^{-}$ *met4*Δ::NatMX *tup1-G2095T*[a]	This study
DBY11406	MATα *hap1*$^{-}$ *met4*Δ::NatMX *dot6-C293A*[a]	This study
DBY12225	MATa/α *HAP1*$^{+}$/*HAP1*$^{+}$ *met4*Δ::KanMX/*MET4 opi1*Δ:: NatMX/*OPI1*	This study
DBY12226	MATa *HAP1*$^{+}$ *met4*Δ:: NatMX *opi1*Δ::KanMX	This study
DBY12227	MAT α *HAP1*$^{+}$ *met4*Δ:: NatMX *opi1*Δ::KanMX	This study
DBY12228	MATa/α *HAP1*$^{+}$/*HAP1*$^{+}$ *met4*Δ::NatMX/*MET4* KanMX::*GAL1*$_{pr}$*-INO1/INO1*	This study
DBY12229	MATa/α *HAP1*$^{+}$/*HAP1*$^{+}$ *met4*Δ::KanMX/*MET4 opi1*Δ::NatMX/*OPI1 ino1*Δ::HphMX4/*INO1*	This study
DBY12230	MATa/α *HAP1*$^{+}$/*HAP1*$^{+}$ *met4*Δ::NatMX/*MET4* KanMX::*GAL1*$_{pr}$*-MUP1/MUP1*	This study
DBY12231	MATa/α *HAP1*$^{+}$/*HAP1 met4*Δ::NatMX/*MET4* KanMX::*GAL1*$_{pr}$*-MUP3/MUP3*	This study
DBY12232	MATa/α *HAP1*$^{+}$/*HAP1*$^{+}$ *met4*Δ::KanMX/*MET4 tup1*Δ::NatMX/*TUP1*	This study
DBY12233	MATa/α *HAP1*$^{+}$/*HAP1 met4*Δ::NatMX/*MET4* KanMX::*GAL1*$_{pr}$*-SAM2/SAM2*	This study
DBY12049	MATa *HAP1 gal1*Δ::*GAL1*$_{pr}$-TEV::HphMX4 *leu2*Δ*0*::*ACT1*$_{pr}$-GEV::NatMX *gal4*Δ::*LEU2*	McIsaac *et al.* (2011)
DBY12055	MATa *HAP1 gal1*Δ::*GAL1*$_{pr}$-TEV::HphMX4 *leu2*Δ*0*::*ACT1*$_{pr}$-GEV::NatMX *gal4*Δ::*LEU2 NDeg-MET4-13Xmyc*::KanMX	McIsaac *et al.* (2011)
DBY12074	MATa *HAP1 gal1*Δ::*GAL1*$_{pr}$-TEV::HphMX4 *leu2*Δ*0*::*ACT1*$_{pr}$-GEV::NatMX *gal4*Δ::*LEU2 NDeg-MET4-13Xmyc*::KanMX *opi1*Δ::KanMX	This study
CC849-8A	MATa *ade2-1 his3-1,15 leu2-3112 trp1-1 ura3 met4*Δ::*TRP1*	Rouillon *et al.* (2000)[c,d]
CC849-1B	MATa *ade2-1 his3-1,15 leu2-3112 trp1-1 ura3 met4*Δ::*TRP1*	Barbey *et al.* (2005)[c]
yMT-234	MATα *ade2-1 can1-100 his3-1,15 leu2-3112 trp1-1 ura3*	K. Nasmyth[c]

[a]Refers to the nucleotide change relative to the ATG.
[b]The exact *opi1* mutation is not known, but sequencing evidence suggests that there is a genomic arrangement.
[c]These strains are in the W303 genetic background.
[d]We found that this strain is MATa, in contrast to the reported MAT (Rouillon *et al.*, 2000).

TABLE 3: Strains used in this study.

liquid media were plated upon completion to check for growth suppression of the *met4*Δ growth defect.

Mutation analysis

Suppressor strains were colony purified by plating and then grown overnight in liquid YPD. Genomic DNA was isolated from saturated cultures using a Qiagen (Valencia, CA) Genomic DNA kit and prepared for hybridization to high-density, whole-genome tiling arrays (GeneChip *S. cerevisiae* Tiling 1.0R; Affymetrix, Santa Clara, CA), as described previously (Gresham *et al.*, 2006). The hybridization data were processed by the SNP Scanner program, which calculated the probability of a mutation at each nucleotide in the genome. These data were visualized using Integrated Genome Browser (http://bioviz.org/igb/) to determine mutations that were specific to *met4*Δ suppressor strains compared with a reference (FY4) and parental strains (DBY12000 and DBY12001).

Estradiol-induction mRNA abundance–time courses

A single colony of *NDeg-MET4*, *opi1*Δ *NDeg-MET4*, or the control strain was grown to mid-log phase. Estradiol was added to a final concentration of 1 μM or 10 nM, and 5-ml aliquots of culture were filtered and flash-frozen in liquid nitrogen at 0 (immediately before estradiol addition), 5, 15, 30, 60, 120, 180, and 360 min after estradiol addition. RNA was isolated using standard phenol:chloroform extraction, purified using an RNeasy RNA purification kit (Qiagen), labeled using the QuickAmp labeling kit (Agilent, Santa Clara, CA), hybridized to 8 × 15k Yeast Aligent Oligo V2 microarrays using Agilent reagents and protocols, washed, and scanned as described (Brauer *et al.*, 2005).

Expression data analysis

All expression data (for both 1 μM and 10 nM estradiol) are provided in Supplemental Data Set S1 and are available in the Princeton University MicroArray database (http://puma.princeton.edu). Expression data were processed as described (Petti *et al.*, 2011) in order to select genes whose time dependence is statistically significant ($p \leq 0.05$) and whose maximum fold change is at least 1.5 in any of the three strains. We also included genes with no time dependence if they showed constitutive differences in expression among the strains (analysis of variance q value ≤ 0.1; Storey and Tibshirani, 2003). To focus our analysis on the most direct effects of Met4p degradation, we used data from the first 30 min (during which the known Met4p targets reached their maximum level of repression) in subsequent processing steps. We also measured gene expression in the same three strains using 10 nM estradiol. These data were used to check each gene for qualitative consistency across different doses of estradiol but were not used in quantitative analyses because other work in our lab showed that 1 μM estradiol is saturating for the estradiol-induction machinery (McIsaac *et al.*, 2011). Genes meeting the foregoing criteria were hierarchically clustered using the MultiExperiment Viewer (Saeed *et al.*, 2006; Supplemental Figure S7) and used as a starting point for the analyses to be described.

Classification of transcription factor dependence

Multiple regression was used to determine whether each gene depends on Met4p, Opi1p, or both. *NDeg-MET4* was compared with the control using the regression model in Eq. 1A, and *opi1*Δ *NDeg-MET4* was compared with *NDeg-MET4* using the regression model in Eq. 1B. In Eq. 1A, the dummy variable D_M classifies the strain as an *NDeg-MET4* strain or a control strain ($D_M = 1$ for *NDeg-MET4*; $D_M = 0$ for control). In Eq. 1B, the dummy variable D_o classifies the strain as an *opi1*Δ *NDeg-MET4* strain or an *NDeg-MET4* strain ($D_o = 1$ for *opi1*Δ *NDeg-MET4*; $D_o = 0$ for *NDeg-MET4*). Regression significance was calculated from the F statistic comparing the fit of the full model (Eq. 1A or Eq. 1B) to the fit of the reduced model (Eq. 1C).

Regression model for dependence on Met4p:

$$Y(t) = \beta_0 + \beta_1 t + \beta_2 t^2 + \beta_3 D_M + \beta_4 D_M t + \beta_5 D_M t^2 \quad (1A)$$

Regression model for dependence on Opi1p:

$$Y(t) = \beta_0 + \beta_1 t + \beta_2 t^2 + \beta_3 D_o + \beta_4 D_o t + \beta_5 D_o t^2 \quad (1B)$$

Reduced regression model:

$$Y(t) = \beta_0 + \beta_1 t + \beta_2 t^2 \quad (1C)$$

A gene was defined as uniquely Met4p dependent (or uniquely Opi1p dependent) if it 1) exhibited statistically significant strain specificity in 1A but not 1B (1B but not 1A), using the F-statistic q value as a measure of significance ($q \leq 0.1$, $p \leq 0.033$), or 2) exhibited constitutively different expression from the comparison strain, using the *t*-test q value as a measure of significance ($q \leq 0.1$, $p \leq 0.0014$). Because the expression profiles of some genes did not fit well to any quadratic, we also included a small number of genes whose expression differed between the strains by a factor of at least two at one or more time points, as long as expression pattern was consistent in both the 1 μM and 10 nM data sets. A gene was defined as jointly dependent on both Met4p and Opi1p if it exhibited strain specificity in both comparisons. We also analyzed genes that were Opi1p regulated but not uniquely so. (These exhibited statistically significant strain specificity in comparison 1B, without regard to comparison 1A.)

Accurately representing time-dependent data using heat maps

We introduce here a new method for representing unevenly sampled gene expression time-course data using heat maps. As in this study, it is common practice to sample biological time courses unevenly, such that measurements are taken more frequently when the variable of interest is changing most quickly. Although heat maps represent high-throughput expression data with unparalleled convenience and conciseness, they misrepresent the time dependence of unevenly sampled data. As a result, visual inspection of heat maps often leads to incorrect conclusions about expression dynamics. Scatterplots, on the other hand, represent time dependence accurately but are not amenable to high-throughput analysis and concise representation (e.g., of hierarchically clustered genes). We combined the best features of both graphical methods by linearly interpolating our unevenly sampled gene expression data and representing the interpolated data using a heat map. As a result, each pair of data points (either real or interpolated) is separated by the same time interval, and the dynamic changes in gene expression are displayed accurately. These interpolated values are only for display in Figures 4 and 5 and are not included in any of our statistical analyses.

Functional enrichment analysis

The functional enrichment of all gene clusters was measured with respect to the functional categorization of yeast genes in the Gene Ontology (http://www.geneontology.org; Ashburner *et al.*, 2000). Enrichment for Gene Ontology terms was measured using the Generic Gene Ontology Term Finder (Boyle *et al.*, 2004) available at

http://go.princeton.edu/cgi-bin/GOTermFinder. Here we used the FDR option for multiple hypothesis correction and only report enrichments with FDR ≤ 0.1. The results of these analyses are shown in Supplemental Data Set S2.

ACKNOWLEDGMENTS

We thank Ryan Briehof for technical help. This work was supported by National Institutes of Health grants GM046406 to D.B. and P50GM071508 to the Center for Quantitative Biology at Princeton University and by the National Science Foundation Research Fellowship Program to R.S.M.

REFERENCES

Aranda A, del Olmo ML (2004). Exposure of *Saccharomyces cerevisiae* to acetaldehyde induces sulfur amino acid metabolism and polyamine transporter genes, which depend on Met4p and Haa1p transcription factors, respectively. Appl Environ Microbiol 70, 1913–1922.

Ashburner M *et al*. (2000). Gene Ontology: tool for the unification of biology. The Gene Ontology Consortium. Nat Genet 25, 25–29.

Ausubel FM (2001). Current Protocols in Molecular Biology, New York: John Wiley & Sons.

Barbey R, Baudouin-Cornu P, Lee TA, Rouillon A, Zarzov P, Tyers M, Thomas D (2005). Inducible dissociation of SCF(Met30) ubiquitin ligase mediates a rapid transcriptional response to cadmium. EMBO J 24, 521–532.

Bihlmaier K, Mesecke N, Terziyska N, Bien M, Hell K, Herrmann JM (2007). The disulfide relay system of mitochondria is connected to the respiratory chain. J Cell Biol 179, 389–395.

Boyle EI, Weng S, Gollub J, Jin H, Botstein D, Cherry JM, Sherlock G (2004). GO::TermFinder—open source software for accessing Gene Ontology information and finding significantly enriched Gene Ontology terms associated with a list of genes. Bioinformatics 20, 3710–3715.

Brachmann CB, Davies A, Cost GJ, Caputo E, Li J, Hieter P, Boeke JD (1998). Designer deletion strains derived from *Saccharomyces cerevisiae* S288C: a useful set of strains and plasmids for PCR-mediated gene disruption and other applications. Yeast 14, 115–132.

Brauer MJ, Saldanha AJ, Dolinski K, Botstein D (2005). Homeostatic adjustment and metabolic remodeling in glucose-limited yeast cultures. Mol Biol Cell 16, 2503–2517.

Carter Z, Delneri D (2010). New generation of loxP-mutated deletion cassettes for the genetic manipulation of yeast natural isolates. Yeast 27, 765–775.

Chandrasekaran S, Deffenbaugh AE, Ford DA, Bailly E, Mathias N, Skowyra D (2006). Destabilization of binding to cofactors and SCFMet30 is the rate-limiting regulatory step in degradation of polyubiquitinated Met4. Mol Cell 24, 689–699.

Chen M, Hancock LC, Lopes JM (2007). Transcriptional regulation of yeast phospholipid biosynthetic genes. Biochim Biophys Acta 1771, 310–321.

Chin J, Bloch K (1988). Phosphatidylcholine synthesis in yeast. J Lipid Res 29, 9–14.

Fauchon M, Lagniel G, Aude JC, Lombardia L, Soularue P, Petat C, Marguerie G, Sentenac A, Werner M, Labarre J (2002). Sulfur sparing in the yeast proteome in response to sulfur demand. Mol Cell 9, 713–723.

Flick K, Ouni I, Wohlschlegel JA, Capati C, McDonald WH, Yates JR, Kaiser P (2004). Proteolysis-independent regulation of the transcription factor Met4 by a single Lys 48-linked ubiquitin chain. Nat Cell Biol 6, 634–641.

Giaever G *et al*. (2002). Functional profiling of the *Saccharomyces cerevisiae* genome. Nature 418, 387–391.

Grant CM, MacIver FH, Dawes IW (1996). Glutathione is an essential metabolite required for resistance to oxidative stress in the yeast *Saccharomyces cerevisiae*. Curr Genet 29, 511–515.

Gresham D, Ruderfer DM, Pratt SC, Schacherer J, Dunham MJ, Botstein D, Kruglyak L (2006). Genome-wide detection of polymorphisms at nucleotide resolution with a single DNA microarray. Science 311, 1932–1936.

Herrgard MJ, Lee BS, Portnoy V, Palsson BO (2006). Integrated analysis of regulatory and metabolic networks reveals novel regulatory mechanisms in *Saccharomyces cerevisiae*. Genome Res 16, 627–635.

Hickman MJ, Winston F (2007). Heme levels switch the function of Hap1 of *Saccharomyces cerevisiae* between transcriptional activator and transcriptional repressor. Mol Cell Biol 27, 7414–7424.

Jesch SA, Zhao X, Wells MT, Henry SA (2005). Genome-wide analysis reveals inositol, not choline, as the major effector of Ino2p-Ino4p and unfolded protein response target gene expression in yeast. J Biol Chem 280, 9106–9118.

Kaiser P, Flick K, Wittenberg C, Reed SI (2000). Regulation of transcription by ubiquitination without proteolysis: Cdc34/SCF(Met30)-mediated inactivation of the transcription factor Met4. Cell 102, 303–314.

Kodaki T, Tsuji S, Otani N, Yamamoto D, Rao KS, Watanabe S, Tsukatsune M, Makino K (2003). Differential transcriptional regulation of two distinct *S*-adenosylmethionine synthetase genes (SAM1 and SAM2) of *Saccharomyces cerevisiae*. Nucleic Acids Res Suppl, 303–304.

Komachi K, Johnson AD (1997). Residues in the WD repeats of Tup1 required for interaction with alpha2. Mol Cell Biol 17, 6023–6028.

Kuras L, Cherest H, Surdin-Kerjan Y, Thomas D (1996). A heteromeric complex containing the centromere binding factor 1 and two basic leucine zipper factors, Met4 and Met28, mediates the transcription activation of yeast sulfur metabolism. EMBO J 15, 2519–2529.

Kuras L, Rouillon A, Lee T, Barbey R, Tyers M, Thomas D (2002). Dual regulation of the met4 transcription factor by ubiquitin-dependent degradation and inhibition of promoter recruitment. Mol Cell 10, 69–80.

Kuras L, Thomas D (1995). Identification of the yeast methionine biosynthetic genes that require the centromere binding factor 1 for their transcriptional activation. FEBS Lett 367, 15–18.

Lee TA, Jorgensen P, Bognar AL, Peyraud C, Thomas D, Tyers M (2010). Dissection of combinatorial control by the Met4 transcriptional complex. Mol Biol Cell 21, 456–469.

Leroy C, Cormier L, Kuras L (2006). Independent recruitment of mediator and SAGA by the activator Met4. Mol Cell Biol 26, 3149–3163.

Loewen CJ, Gaspar ML, Jesch SA, Delon C, Ktistakis NT, Henry SA, Levine TP (2004). Phospholipid metabolism regulated by a transcription factor sensing phosphatidic acid. Science 304, 1644–1647.

Loewen CJ, Levine TP (2005). A highly conserved binding site in vesicle-associated membrane protein-associated protein (VAP) for the FFAT motif of lipid-binding proteins. J Biol Chem 280, 14097–14104.

Longtine MS, McKenzie A 3rd, Demarini DJ, Shah NG, Wach A, Brachat A, Philippsen P, Pringle JR (1998). Additional modules for versatile and economical PCR-based gene deletion and modification in *Saccharomyces cerevisiae*. Yeast 14, 953–961.

MacIsaac KD, Wang T, Gordon DB, Gifford DK, Stormo GD, Fraenkel E (2006). An improved map of conserved regulatory sites for *Saccharomyces cerevisiae*. BMC Bioinformatics 7, 113.

Malanovic N, Streith I, Wolinski H, Rechberger G, Kohlwein SD, Tehlivets O (2008). S-adenosyl-L-homocysteine hydrolase, key enzyme of methylation metabolism, regulates phosphatidylcholine synthesis and triacylglycerol homeostasis in yeast: implications for homocysteine as a risk factor of atherosclerosis. J Biol Chem 283, 23989–23999.

Malave TM, Dent SY (2006). Transcriptional repression by Tup1-Ssn6. Biochem Cell Biol 84, 437–443.

Masselot M, De Robichon-Szulmajster H (1975). Methionine biosynthesis in *Saccharomyces cerevisiae*. I. Genetical analysis of auxotrophic mutants. Mol Gen Genet 139, 121–132.

McCammon MT, Hartmann MA, Bottema CD, Parks LW (1984). Sterol methylation in *Saccharomyces cerevisiae*. J Bacteriol 157, 475–483.

McGraw P, Henry SA (1989). Mutations in the *Saccharomyces cerevisiae* opi3 gene: effects on phospholipid methylation, growth and cross-pathway regulation of inositol synthesis. Genetics 122, 317–330.

McIsaac RS, Silverman SJ, McClean MN, Gibney PA, Macinskas J, Hickman MJ, Petti A, Botstein D (2011). Fast-acting and nearly gratuitous induction of gene expression and protein depletion in *Saccharomyces cerevisiae*. Mol Biol Cell (*in press*).

Mountain HA, Bystrom AS, Korch C (1993). The general amino acid control regulates MET4, which encodes a methionine-pathway-specific transcriptional activator of *Saccharomyces cerevisiae*. Mol Microbiol 7, 215–228.

Nurminen T, Taskinen L, Suomalainen H (1976). Distribution of membranes, especially of plasma-membrane fragments, during zonal centrifugations of homogenates from glucose-repressed *Saccharomyces cerevisiae*. Biochem J 154, 751–763.

Patton EE, Peyraud C, Rouillon A, Surdin-Kerjan Y, Tyers M, Thomas D (2000). SCF(Met30)-mediated control of the transcriptional activator Met4 is required for the G(1)-S transition. EMBO J 19, 1613–1624.

Petti AA, Crutchfield CA, Rabinowitz JD, Botstein D (2011). Survival of starving yeast is correlated with oxidative stress response and nonrespiratory mitochondrial function. Proc Natl Acad Sci USA 2011 Jul 6 [Epub ahead of print].

Reed SI, Hadwiger JA, Lorincz AT (1985). Protein kinase activity associated with the product of the yeast cell division cycle gene CDC28. Proc Natl Acad Sci USA 82, 4055–4059.

Rouillon A, Barbey R, Patton EE, Tyers M, Thomas D (2000). Feedback-regulated degradation of the transcriptional activator Met4 is triggered by the SCF(Met30)complex. EMBO J 19, 282–294.

Saeed AI, Bhagabati NK, Braisted JC, Liang W, Sharov V, Howe EA, Li J, Thiagarajan M, White JA, Quackenbush J (2006). TM4 microarray software suite. Methods Enzymol 411, 134–193.

Santiago TC, Mamoun CB (2003). Genome expression analysis in yeast reveals novel transcriptional regulation by inositol and choline and new regulatory functions for Opi1p, Ino2p, and Ino4p. J Biol Chem 278, 38723–38730.

Shetty A, Lopes JM (2010). Derepression of INO1 transcription requires cooperation between the Ino2p-Ino4p heterodimer and Cbf1p and recruitment of the ISW2 chromatin-remodeling complex. Eukaryot Cell 9, 1845–1855.

Sikorski RS, Hieter P (1989). A system of shuttle vectors and yeast host strains designed for efficient manipulation of DNA in *Saccharomyces cerevisiae*. Genetics 122, 19–27.

Snoek IS, Steensma HY (2006). Why does *Kluyveromyces lactis* not grow under anaerobic conditions? Comparison of essential anaerobic genes of *Saccharomyces cerevisiae* with the *Kluyveromyces lactis* genome. FEMS Yeast Res 6, 393–403.

Sprague ER, Redd MJ, Johnson AD, Wolberger C (2000). Structure of the C-terminal domain of Tup1, a corepressor of transcription in yeast. EMBO J 19, 3016–3027.

Sreenivas A, Carman GM (2003). Phosphorylation of the yeast phospholipid synthesis regulatory protein Opi1p by protein kinase A. J Biol Chem 278, 20673–20680.

Storey JD, Tibshirani R (2003). Statistical significance for genomewide studies. Proc Natl Acad Sci USA 100, 9440–9445.

Strathern JN, Jones EW, Broach JR (1982). The Molecular Biology of the Yeast *Saccharomyces*. Metabolism and Gene Expression, Cold Spring Harbor, NY: Cold Spring Harbor Laboratory.

Summers EF, Letts VA, McGraw P, Henry SA (1988). *Saccharomyces cerevisiae* cho2 mutants are deficient in phospholipid methylation and cross-pathway regulation of inositol synthesis. Genetics 120, 909–922.

Thomas D, Jacquemin I, Surdin-Kerjan Y (1992). MET4, a leucine zipper protein, and centromere-binding factor 1 are both required for transcriptional activation of sulfur metabolism in *Saccharomyces cerevisiae*. Mol Cell Biol 12, 1719–1727.

Thomas D, Rothstein R, Rosenberg N, Surdin-Kerjan Y (1988). SAM2 encodes the second methionine S-adenosyl transferase in *Saccharomyces cerevisiae*: physiology and regulation of both enzymes. Mol Cell Biol 8, 5132–5139.

Thomas D, Surdin-Kerjan Y (1987). SAM1, the structural gene for one of the S-adenosylmethionine synthetases in *Saccharomyces cerevisiae*. Sequence and expression. J Biol Chem 262, 16704–16709.

Thomas D, Surdin-Kerjan Y (1997). Metabolism of sulfur amino acids in *Saccharomyces cerevisiae*. Microbiol Mol Biol Rev 61, 503–532.

Tong AH *et al.* (2001). Systematic genetic analysis with ordered arrays of yeast deletion mutants. Science 294, 2364–2368.

Wagner C, Dietz M, Wittmann J, Albrecht A, Schuller HJ (2001). The negative regulator Opi1 of phospholipid biosynthesis in yeast contacts the pleiotropic repressor Sin3 and the transcriptional activator Ino2. Mol Microbiol 41, 155–166.

Wheeler GL, Quinn KA, Perrone G, Dawes IW, Grant CM (2002). Glutathione regulates the expression of gamma-glutamylcysteine synthetase via the Met4 transcription factor. Mol Microbiol 46, 545–556.

White MJ, Hirsch JP, Henry SA (1991). The OPI1 gene of *Saccharomyces cerevisiae*, a negative regulator of phospholipid biosynthesis, encodes a protein containing polyglutamine tracts and a leucine zipper. J Biol Chem 266, 863–872.

Winston F, Dollard C, Ricupero-Hovasse SL (1995). Construction of a set of convenient *Saccharomyces cerevisiae* strains that are isogenic to S288C. Yeast 11, 53–55.

Zomorrodi AR, Maranas CD (2010). Improving the iMM904 S. cerevisiae metabolic model using essentiality and synthetic lethality data. BMC Syst Biol 4, 178.